COMMUNICATION

Check for updates

High-performing fiber electrodes based on a gold-shelled silver nanowire framework for bioelectronics†

Kailin Zhang,‡ Chengqiang Tang,‡ Sihui Yu, Hang Guan, Xiao Sun, Mingjie Cao, Songlin Zhang, Xuemei Sun [ID] * and Huisheng Peng [ID]

Flexible fiber electrodes offer new opportunities for bioelectronics and are reliable *in vivo* applications, high flexibility, high electrical conductivity, and satisfactory biocompatibility are typically required. Herein, we present an all-metal flexible and biocompatible fiber electrode based on a metal nanowire hybrid strategy, *i.e.*, silver nanowires were assembled on a freestanding framework, and further to render them inert, they were plated with a gold nanoshell. Our fiber electrodes exhibited a low modulus of $\sim$75 MPa and electrical conductivity up to $\sim$4.8 $\times$ 10^6 S m^{-1}. They can resist chemical erosion with negligible leakage of biotoxic silver ions in the physiological environment, thus ensuring satisfactory biocompatibility. Finally, we demonstrated the hybrid fiber as a neural electrode that stimulated the sciatic nerve of a mouse, proving its potential for applications in bioelectronics.

1. Introduction

Fiber electrodes have facilitated the development of bioelectronics to drive progress in biology, such as in neuroscience.[1–3] They build bridges to connect biology and external electronics, and enable signal acquisition from tissues to understand the biology and stimulate delivery from external electronics to modulate the tissues.[4] To ensure that this bridge is stable and reliable, fiber electrodes should possess the qualities of high electrical conductivity for signal transmission efficiency, high flexibility to match with soft tissue, and biocompatibility.[5–8]

For these requirements, metal wires are the most conductive, but they are highly rigid.[9] Therefore, new strategies have been developed to form composites of metal nanomaterials with low-modulus polymers, such as compositing silver nanowires (AgNWs) with elastomer fibers to obtain flexibility. Still, their conductivities exponentially decrease,[10] while the AgNWs will erode and leak Ag$^+$ in the physiological environment, leading to severe toxicity to tissue.[11] Although there are other fiber electrodes based on polymers and carbon materials that exhibit satisfactory flexibility and biocompatibility, their conductivities are much lower than those of metals,[12] which limits the improvement of bioelectronics.[13]

Herein, we propose a strategy of using the AgNWs to build network structures and depositing inert gold nanoshells on their surface to prepare hybrid (Au@AgNW) fibers (Fig. 1a). This hybrid strategy combines the high electrical conductivity of the AgNWs and satisfactory biocompatibility of a gold layer without breaking the network structure constructed by the AgNWs. The network structure provides Au@AgNW fibers with high flexibility, *e.g.*, the modulus is as low as $\sim$75 MPa. Because of the all-metal composition and effective connection among nanowires, their electrical conductivity can be as high as $\sim$4.8 $\times$ 10^6 S m^{-1}, which is comparable to that of dense metal fiber electrodes. Moreover, the gold nanoshell acts as a protective barrier between the AgNWs and physiological environment, effectively shielding silver from chemical erosion by hydrogen peroxide and halogen ions, as well as preventing the leakage of Ag$^+$. This ensures electrochemical stability and biocompatibility of the electrode. As a proof-of-concept, we demonstrate that the fiber can act as a neural electrode to stimulate the sciatic nerve of a mouse, showing its potential for applications in bioelectronics.

2. Results and discussions

2.1 Preparation of the Au@AgNW fibers

One-dimensional conductive nanomaterials can be assembled with disorder to provide a balance between flexibility and conductivity.[14] Thus, a suspension of the AgNWs was sprayed

State Key Laboratory of Molecular Engineering of Polymers, Department of Macromolecular Science, Institute of Fiber Materials and Devices, and Laboratory of Advanced Materials, Fudan University, Shanghai 200438, China.
E-mail: sunxm@fudan.edu.cn

5594 | *J. Mater. Chem. B,* 2024, **12**, 5594–5599

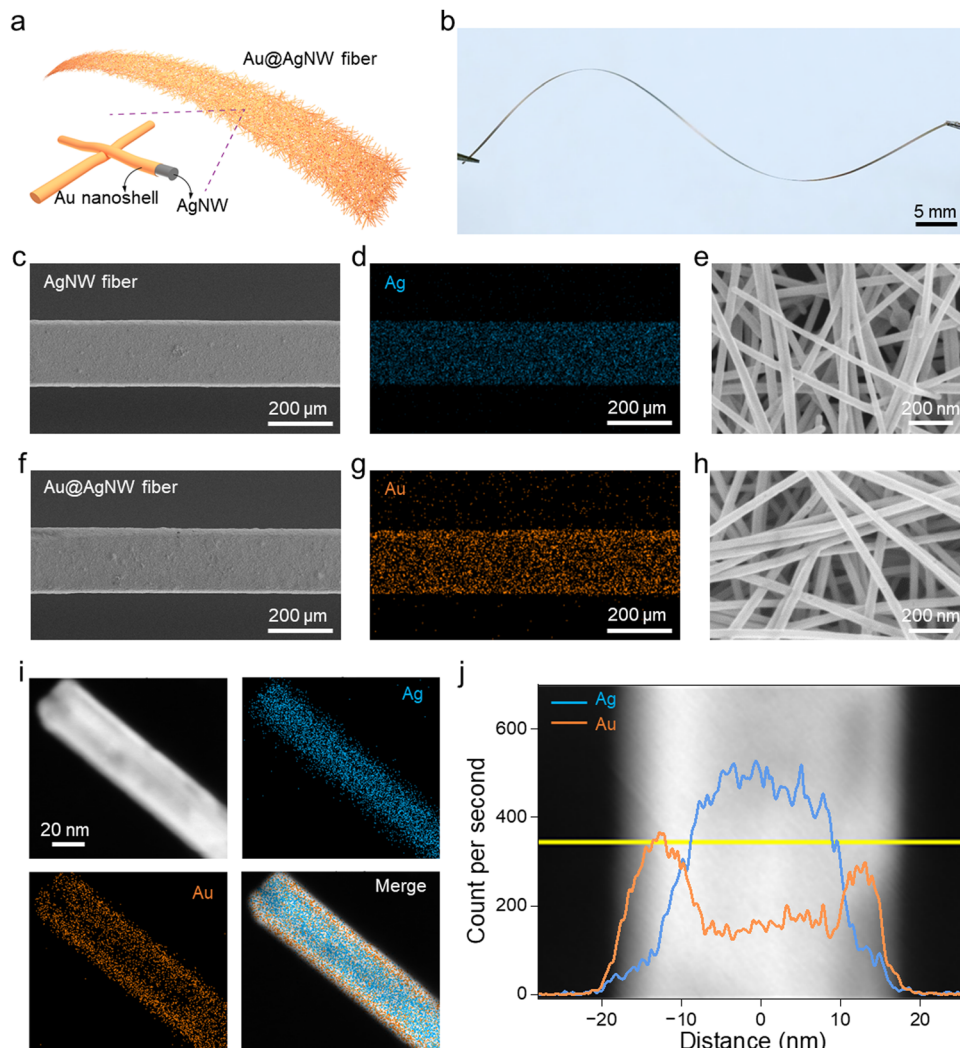This journal is © The Royal Society of Chemistry 2024

Fig. 1 Structure and morphology of the Au@AgNW fibers. (a) Schematic diagram of the Au@AgNW fibers. (b) Photograph of a twisted Au@AgNW fiber. (c) Scanning electron microscopy (SEM) image, (d) element distribution, and (e) high-magnification SEM image of the AgNW fiber. (f) SEM image, (g) element distribution, and (h) high-magnification SEM image of the Au@AgNW fiber. (i) TEM image and element distribution of a single nanowire in the Au@AgNW fiber. (j) Line scan results of the radial element distribution of a single nanowire. The background shows a TEM image of the sampled nanowire, and the yellow line marks the scanning path.

onto a polyethylene terephthalate sheet and patterned with a mask plate. Subsequently, the solvent was rapidly evaporated to obtain primary fibers with internal AgNWs in contact with each other. Then, the dispersion stabilizer polyvinylpyrrolidone on the surface of the AgNWs was desorbed in the calcium chloride solution, and the overlapping points of the AgNWs were chemically sintered as mutual diffusion bonding occurred[15,16] (Fig. S1–S3, ESI†). Sintered fibers were structurally stable, and with the volatilization of ethanol, they detached from polyethylene terephthalate sheets and were self-supporting.

To optimize their chemical stability, a mild galvanic-free deposition strategy was used to uniformly coat the AgNW fibers with a chemically stable gold shell.[17] During this process, SO_3^{2-} in the gold seed solution was bound with Au^{3+} to decrease the reduction potential of Au^{3+}. The binding can increase the energy barrier of the galvanic coupling substitution reaction to inhibit the direct charge transfer of Au^{3+}, which induces

random deposition on the AgNWs. L-Ascorbic acid in the growth solution was used as the reducing agent, and its reducing velocity could be tuned by changing the pH, which would inhibit the galvanic replacement reaction.[18] As a result, Au^{3+} was controlled to homogeneously nucleate on the AgNW surface to form a uniform and dense gold shell (Fig. S4, ESI†),[19] resulting in flexible Au@AgNW fibers.

2.2 Structure, electrical, and mechanical properties of the Au@AgNW fibers

The color of the AgNW fibers changed from gray to deep yellow after hybridizing with a gold shell (Fig. S5, ESI†), and the Au@AgNW fiber was self-supporting. It was able to withstand bending and twisting (Fig. 1b). The AgNW fiber and Au@AgNW fiber shared the same flat surface and anisotropically arranged a nanowire network structure without bundle aggregation. Energy dispersive X-ray spectroscopy results and high

magnification scanning electron microscopy (SEM) images show that the surface of the Au@AgNW fiber was entirely covered by a continuous dense gold shell (Fig. 1c–h and Fig. S6, ESI†). Notably, sintered points between adjacent nanowires were maintained to ensure that structural stability and a conductive pathway were established. High-resolution transmission electron microscopy was used to observe a single nanowire in the Au@AgNW fiber, and a homogeneous AgNW core and gold shell structure was observed (Fig. 1i). The distribution statistics of the relative content of elements in the radial direction of the nanowire showed a uniform gold shell with a thickness of $\sim$4 nm (Fig. 1j).

Due to the porous nanowire network structure inside the Au@AgNW fiber, it exhibited flexibility far superior to that of dense silver. Nanoindentation results showed that the effective elastic modulus of the Au@AgNW fiber was $\sim$75 MPa, which was only $\sim$1/130 of that of dense silver (Fig. 2a and b). This structure also enabled it to be easily bent, with stronger compliance than dense silver of the same size (Fig. 2c). Because of the continuous network based on all-metal nanowires and stable sintered points, the Au@AgNW fibers exhibited a high electrical conductivity up to $\sim$4.8 $\times$ 10^6 S m^{-1}, which was much higher than many existing flexible fiber electrodes in which non-conductive components must be incorporated[10,20–29] (Fig. 2d). The mechanical stability under cyclic bending and twisting of the Au@AgNW fibers was satisfactory, without any significant increase in resistance (Fig. S7, ESI†). Furthermore, the rich nanostructure led to a high specific surface area that enabled a stronger electrochemical performance compared to dense metals, and it was suitable for *in vivo* applications such as electrical stimulation due to its higher charge injection capability (Fig. 2e).

2.3 Chemical and electrochemical stability of the Au@AgNW fibers

Considering the chemical instability to which electrode materials are subject when working *in vivo*, hydrogen peroxide solution, calcium chloride solution, and ozone were used to examine the ability of the gold nanoshells to protect against the AgNWs in the Au@AgNW fiber.[19] Hydrogen peroxide participates in many physiological reactions, such as the glucose conversion process. It can be catalyzed by the AgNWs to decompose and release oxygen, leading to chemical erosion of the AgNWs.[30] Cl$^-$ is a vital component of body fluids that plays a crucial role in maintaining the electrolyte balance and cell membrane osmotic pressure, and it is directly involved in neuronal firing processes.[31] Given the strong binding affinity of Cl$^-$ to Ag$^+$, they can induce the etching or dissolution of silver.[32] Ozone was used to accelerate the simulated air contact oxidation process.[33]

We first evaluated the integrity of the conductive network in fibers by monitoring their resistance changes ($\Delta R/R_0$) when subjected to a chemical environment for 24 h. For the AgNW fiber group, the $\Delta R/R_0$ significantly changed after 1 h and finally reached approximately 2. The $\Delta R/R_0$ increased to $\sim$15 in calcium chloride solution and $\sim$90 under ozone because corrosion occurred with greater severity. After being protected
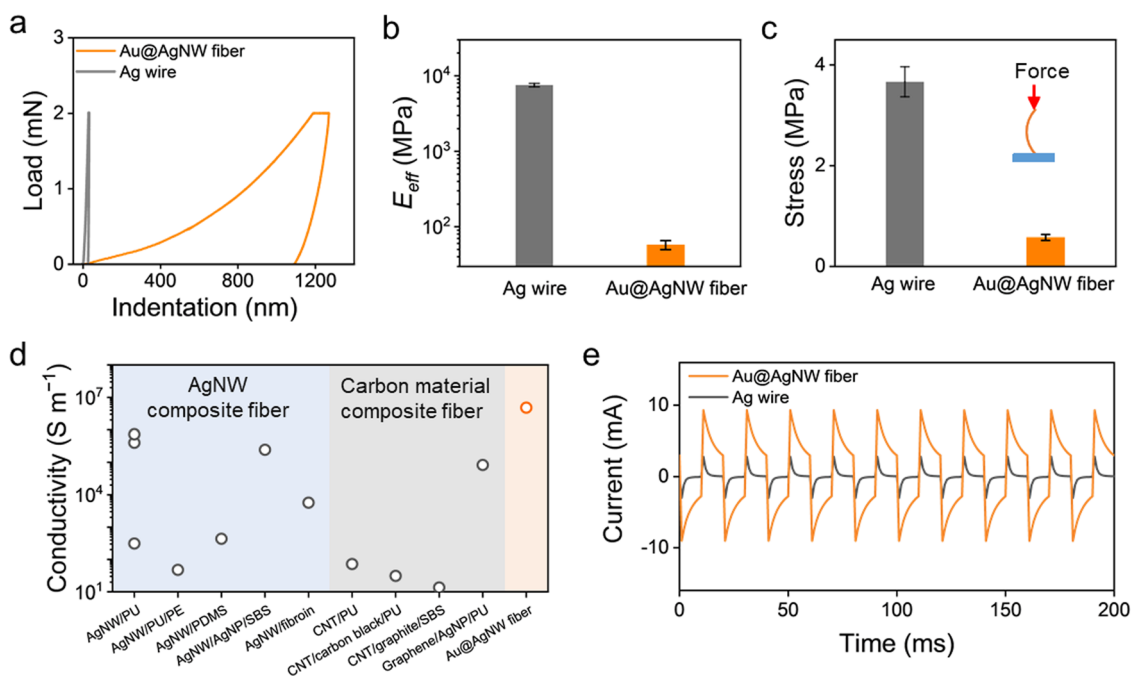

Fig. 2 Mechanical, electrical, and electrochemical properties of the Au@AgNW fibers. (a) Load−displacement curves from indentation tests of the Au@AgNW fiber and Ag wire. (b) Effective elastic moduli and (c) maximum bending stress of the Au@AgNW fibers and Ag wires (N = 3). (d) Comparison of the conductivity between the Au@AgNW fiber and other flexible fiber electrodes. PU: polyurethane; PE: polyethylene; PDMS: polydimethylsiloxane; SBS: styrene−butadiene−styrene's block copolymers; AgNP: silver nanoparticle; CNT: carbon nanotube. (e) Current generation by the Au@AgNW fiber and Ag wire upon applying ±0.5 V bipolar pulses with a frequency of 50 Hz. The data in (b) and (c) are shown as the mean ± SD.

5596 | *J. Mater. Chem. B*, 2024, **12**, 5594–5599

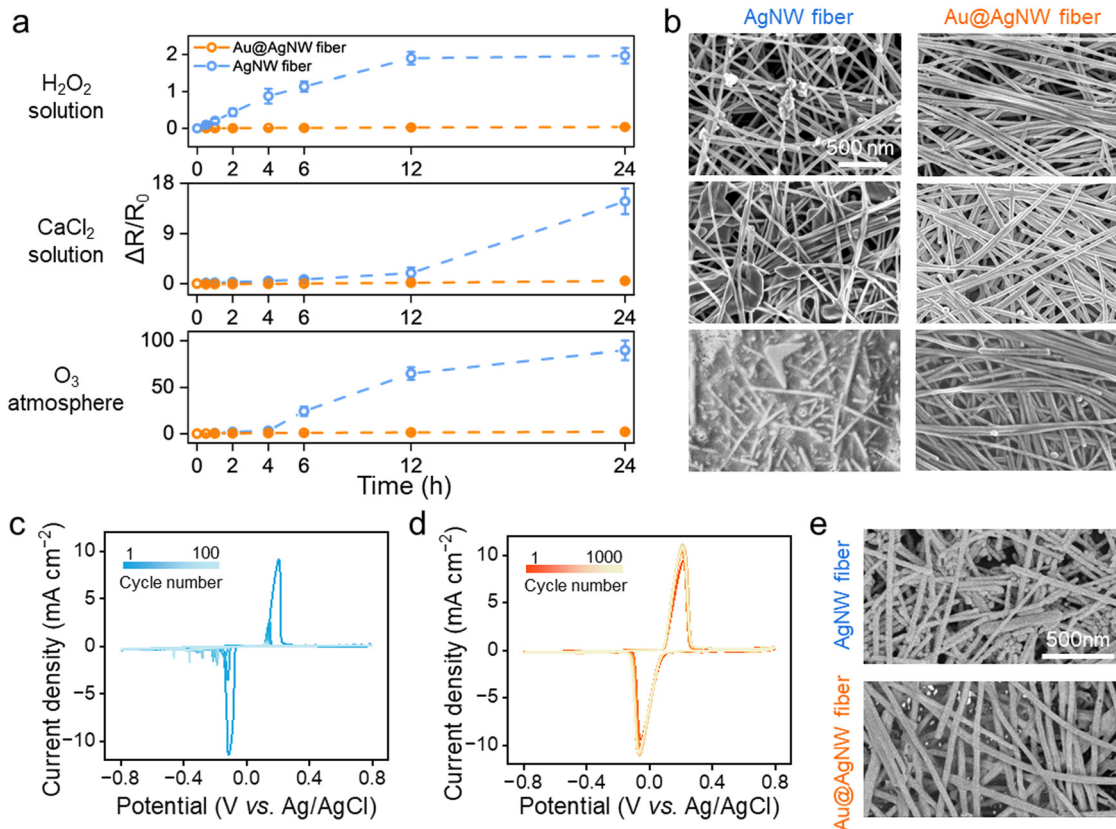This journal is © The Royal Society of Chemistry 2024

Fig. 3 Chemical and electrochemical stability of the Au@AgNW fibers. (a) Resistance changes of the fibers during chemical erosion ($N = 3$). The data are shown as the mean ± SD. (b) SEM images of the fibers after different chemical erosion processes. Cyclic voltammetry curves of the (c) AgNW fiber and (d) Au@AgNW fiber. (e) SEM images of the fibers after cyclic voltammetry scanning, with 100 cycles for the AgNW fiber and 1000 cycles for the Au@AgNW fiber.

by the gold nanoshell, the Au@AgNW fiber group remained stable in all above-mentioned environments, and the values of $\Delta R/R_0$ were only 0.04 in hydrogen peroxide solution, 0.49 in calcium chloride solution, and 1.99 under an ozone atmosphere (Fig. 3a). The morphologies from SEM showed that hydrogen peroxide induced silver oxide crystals to appear on the AgNWs, calcium chloride caused coarsening of the AgNWs and disrupted the network structure, and ozone directly disintegrated the AgNWs. In contrast, the Au@AgNW fibers maintained their structural integrity (Fig. 3b), as well as their mechanical stability (Fig. S8, ESI†).

Electrochemical reactions are often involved in the operation of bioelectronic devices. Therefore, it is necessary to consider the electrochemical stability of fiber electrodes.[34] Cyclic voltammetry results showed that the bare AgNW fiber lost its reversible redox ability after a few cycles (Fig. 3c), whereas the Au@AgNW fiber maintained a stable reversible redox ability after 1000 cycles (Fig. 3d). SEM images also showed that the structure of the Au@AgNW fiber was stable after the above process (Fig. 3e). These results prove that the Au@AgNW fiber is capable of enduring electrochemical processes in physiological environments.

Furthermore, the fiber electrodes were immersed in a 1× PBS solution to simulate an *in vivo* liquid environment, and the Ag⁺ concentration in the solution was measured at different time points. The results showed that the AgNW fibers continuously released Ag⁺

into the solution, with a concentration of 174.7 μg L^{-1} after 7 days. However, the Au@AgNW fiber group showed an Ag⁺ concentration of less than 1/10 of that in the AgNW fiber group because the gold nanoshell significantly slowed the leakage of Ag⁺ (Fig. S9, ESI†). Therefore, chemical reactions between Ag⁺ and functional groups such as sulfur groups or carboxyl groups in protein can be inhibited, which potentially increases the safety *in vivo*.[35]

2.4 Biocompatibility and *in vivo* applications

We systematically evaluated the biocompatibility of the Au@AgNW fibers from the cellular to the tissue level. Mouse fibroblasts were cultured with the AgNW fibers and Au@AgNW fibers as substrates for 72 h. The AgNW fiber was significantly oxidized, with spherical silver oxide particles appearing on the surface that exhibited a large amount of structural coarsening. In contrast, there was no significant structural change in the Au@AgNW fiber group (Fig. S10, ESI†), and the Au@AgNW fiber did not affect the cell morphology (Fig. S11, ESI†). Furthermore, CCK-8 was used to characterize cell proliferation and toxicity. The results showed that the AgNW fibers inhibited cell proliferation, and the number of cells was only 51% of that of the control group. In contrast, the Au@AgNW fiber group exhibited negligible toxicity compared to the control group (Fig. 4a).

Furthermore, the fiber electrodes were implanted into the subcutaneous tissues of mice, and Ag⁺ concentrations in

This journal is © The Royal Society of Chemistry 2024

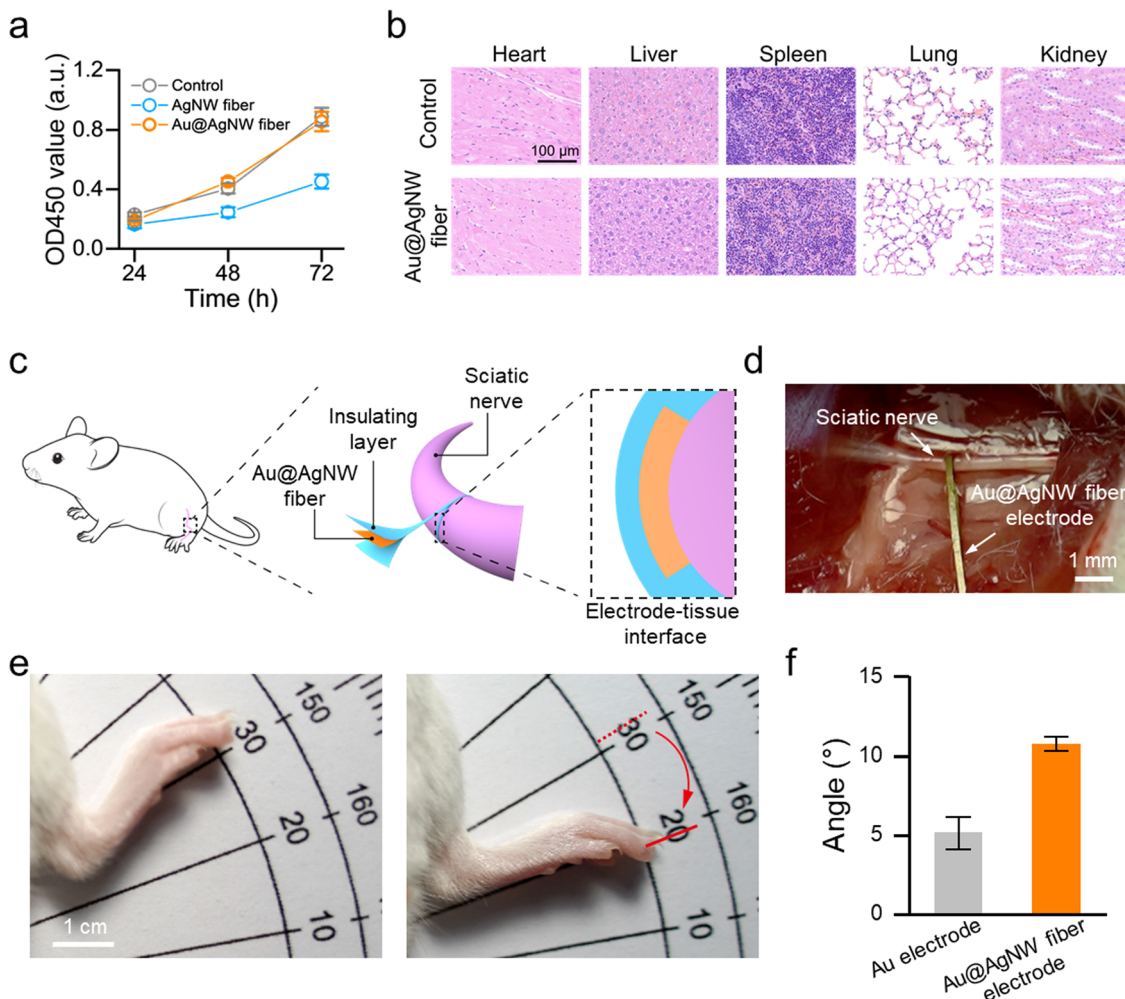*J. Mater. Chem. B*, 2024, **12**, 5594–5599 | **5597**

Fig. 4 Biocompatibility and *in vivo* applications of the Au@AgNW fibers. (a) Growth curve of L929 mouse fibroblast cells incubated with different fiber substrates (*N* = 5). (b) Hematoxylin–eosin (H&E) staining images of major organs after subcutaneous implantation of the Au@AgNW fibers for 7 days. (c) Diagram and (d) photograph showing that the Au@AgNW fiber electrode can establish conformable contact with the sciatic nerve for electrical stimulation. (e) Electrical stimulation evokes leg movement by the mouse at 1 week after implantation of the Au@AgNW fiber electrode. (f) Comparison of the leg movement induced by bare Au and the Au@AgNW fiber through the same electrical stimulation at 1 week after implantation (*N* = 3). The data in a and f are shown as the mean ± SD.

surrounding tissues were measured after implantation for 7 days. The results showed that the average value of Ag^+ concentration in the AgNW fiber group was ~ 4.0 mg kg^{-1}. The value in the Au@AgNW fiber group was only ~ 0.4 mg kg^{-1} (Fig. S12, ESI†). No structural damage was observed in the Au@AgNW fibers (Fig. S13, ESI†). These indicated that the Au@AgNW fiber can stably and safely operate *in vivo*. This was further confirmed by the results of hematoxylin–eosin staining of the heart, liver, spleen, lungs, and kidneys of mice implanted with the Au@AgNW fibers, in which no obvious tissue inflammation or lesions was found compared with the control group (Fig. 4b).

To demonstrate the actual application *in vivo*, the Au@AgNW fibers were used as neural electrodes for electrical stimulation of the sciatic nerve in mice (Fig. 4c). With satisfactory flexibility, they compliantly made contact on the surface of the sciatic nerve, *i.e.*, no obvious gaps between them and deformation of the nerve were observed[36] (Fig. 4d). The mouse regressed with a significant leg movement in response to bipolar pulses. Compared with conventional dense Au electrodes, Au@AgNW fiber electrodes induced a larger angle of leg movement under the same electrical stimulation because of the higher charge injection capability derived from nanowire networks[37] (Fig. 4e and f). Furthermore, no damage was observed in the surrounding tissue during chronic implantation (Fig. S14, ESI†). Finally, the excellent chemical stability and biocompatibility of the Au@AgNW fiber allowed the electrode to stably operate *in vivo* for 4 weeks without decay (Fig. S15, ESI†).

3. Conclusion

In conclusion, we have developed highly flexible, conductive, and biocompatible fiber electrodes with a chemically sintered AgNW network as the main framework and a gold nanoshell as the inert layer. The modulus of the fiber was significantly reduced to approximately $\sim 1/130$ of that of dense metals. Additionally, because the incorporation of an inert gold nanoshell ensured excellent chemical and electrochemical stability and biocompatibility, the fibers were able to stably function in complex physiological environments. These fibers and the

5598 | *J. Mater. Chem. B*, 2024, **12**, 5594–5599

This journal is © The Royal Society of Chemistry 2024

metal nanowire hybrid strategy are promising for high-performing bioelectronics. In the future, it will be necessary to develop industrial-scale production for greater uniformity and to lower the cost so that these high-performance hybrid fibers can be applied in additional fields.[38]

Data availability statement

The data that support the findings of this study are available from the corresponding author upon reasonable request.

Conflicts of interest

The authors declare no conflicts of interest.

Acknowledgements

References

1 C. Chen, J. Feng, J. Li, Y. Guo, X. Shi and H. Peng, *Chem. Rev.*, 2023, **123**, 613–662.

2 L. Wei, S. Wang, M. Shan, Y. Li, Y. Wang, F. Wang, L. Wang and J. Mao, *Bioact. Mater.*, 2023, **22**, 343–364.

3 C. Tang, S. Xie, M. Wang, J. Feng, Z. Han, X. Wu, L. Wang, C. Chen, J. Wang, L. Jiang, P. Chen, X. Sun and H. Peng, *J. Mater. Chem. B*, 2020, **8**, 4387–4394.

4 H. Yuk, B. Lu and X. Zhao, *Chem. Soc. Rev.*, 2019, **48**, 1642–1667.

5 S. Park, H. Yuk, R. Zhao, Y. S. Yim, E. W. Woldeghebriel, J. Kang, A. Canales, Y. Fink, G. B. Choi, X. Zhao and P. Anikeeva, *Nat. Commun.*, 2021, **12**, 3435.

6 J. Wang, L. Wang, Y. Yang, H. Li, X. Huang, Z. Liu, S. Yu, C. Tang, J. Chen, X. Shi, W. Li, P. Chen, Q. Tong, H. Yu, X. Sun and H. Peng, *Adv. Mater.*, 2023, **36**, 2309862.

7 Z. Lei, W. Xu and G. Zhang, *Smart Med.*, 2023, **2**, e20220026.

8 C. Liu, K. Peng, Y. Wu and F. Fu, *Smart Med.*, 2023, **2**, e20230024.

9 A. Obaid, M.-E. Hanna, Y.-W. Wu, M. Kollo, R. Racz, M. R. Angle, J. Müller, N. Brackbill, W. Wray, F. Franke, E. J. Chichilnisky, A. Hierlemann, J. B. Ding, A. T. Schaefer and N. A. Melosh, *Sci. Adv.*, 2020, **6**, eaay2789.

10 Y. Lu, J. Jiang, S. Yoon, K.-S. Kim, J.-H. Kim, S. Park, S.-H. Kim and L. Piao, *ACS Appl. Mater. Interfaces*, 2018, **10**, 2093–2104.

11 T. Araki, F. Yoshida, T. Uemura, Y. Noda, S. Yoshimoto, T. Kaiju, T. Suzuki, H. Hamanaka, K. Baba, H. Hayakawa, T. Yabumoto, H. Mochizuki, S. Kobayashi, M. Tanaka, M. Hirata and T. Sekitani, *Adv. Healthcare Mater.*, 2019, **8**, 1900130.

12 Y. Li, K. Zhang, L. Zhang, M. Nie and Q. Wang, *Compos. Sci. Technol.*, 2021, **213**, 108900.

13 J. Wang, L. Wang, J. Feng, C. Tang, X. Sun and H. Peng, *Adv. Fiber Mater.*, 2021, **3**, 47–58.

14 R. J. Headrick, D. E. Tsentalovich, J. Berdegué, E. A. Bengio, L. Liberman, O. Kleinerman, M. S. Lucas, Y. Talmon and M. Pasquali, *Adv. Mater.*, 2018, **30**, 1704482.

15 M. Grouchko, A. Kamyshny, C. F. Mihailescu, D. F. Anghel and S. Magdassi, *ACS Nano*, 2011, **5**, 3354–3359.

16 J. Gu, X. Wang, H. Chen, S. Yang, H. Feng, X. Ma, H. Ji, J. Wei and M. Li, *Nanotechnology*, 2018, **29**, 265703.

17 M. Yang, Z. D. Hood, X. Yang, M. Chi and Y. Xia, *Chem. Commun.*, 2017, **53**, 1965–1968.

18 V. Yadav, S. Jeong, X. Ye and C. W. Li, *Chem. Mater.*, 2022, **34**, 1897–1904.

19 S. Choi, S. I. Han, D. Jung, H. J. Hwang, C. Lim, S. Bae, O. K. Park, C. M. Tschabrunn, M. Lee, S. Y. Bae, J. W. Yu, J. H. Ryu, S.-W. Lee, K. Park, P. M. Kang, W. B. Lee, R. Nezafat, T. Hyeon and D.-H. Kim, *Nat. Nanotech.*, 2018, **13**, 1048–1056.

20 P. Walter, B. Podsiadły, M. Zych, M. Kamiński, A. Skalski, T. Raczyński, D. Janczak and M. Jakubowska, *Sensors*, 2022, **22**, 800.

21 G.-J. Zhu, P.-G. Ren, H. Guo, Y.-L. Jin, D.-X. Yan and Z.-M. Li, *ACS Appl. Mater. Interfaces*, 2019, **11**, 23649–23658.

22 Y. Cheng, R. Wang, J. Sun and L. Gao, *ACS Nano*, 2015, **9**, 3887–3895.

23 Y. Cheng, R. Wang, H. Zhai and J. Sun, *Nanoscale*, 2017, **9**, 3834–3842.

24 L. Ding, S. Xuan, J. Feng and X. Gong, *Composites, Part A*, 2017, **100**, 97–105.

25 S. Lee, S. Shin, S. Lee, J. Seo, J. Lee, S. Son, H. J. Cho, H. Algadi, S. Al-Sayari, D. E. Kim and T. Lee, *Adv. Funct. Mater.*, 2015, **25**, 3114–3121.

26 Y. Lu, J. Jiang, S. Park, D. Wang, L. Piao and J. Kim, *Bull. Korean Chem. Soc.*, 2020, **41**, 162–169.

27 Z. Zhuang, N. Cheng, L. Zhang, L. Liu, J. Zhao and H. Yu, *Nanotechnology*, 2020, **31**, 205701.

28 Z. Zhang, M. T. Innocent, N. Tang, R. Li, Z. Hu, M. Zhai, L. Yang, W. Ma, H. Xiang and M. Zhu, *ACS Appl. Mater. Interfaces*, 2022, **14**, 44832–44840.

29 S.-W. Kim, S.-N. Kwon and S.-I. Na, *Composites, Part B*, 2019, **167**, 573–581.

30 L. Shi, M. Layani, X. Cai, H. Zhao, S. Magdassi and M. Lan, *Sens. Actuators, B*, 2018, **256**, 938–945.

31 V. Patel, A. Mardolkar, A. Shelar, R. Tiwari and R. Srivastava, *Anal. Methods*, 2024, **16**, 1439–1453.

32 Z. Hui, Y. Liu, W. Guo, L. Li, N. Mu, C. Jin, Y. Zhu and P. Peng, *Nanotechnology*, 2017, **28**, 285703.

33 D. C. Choo, S. K. Bae and T. W. Kim, *Sci. Rep.*, 2019, **9**, 5527.

34 L. Wang, S. Xie, Z. Wang, F. Liu, Y. Yang, C. Tang, X. Wu, P. Liu, Y. Li, H. Saiyin, S. Zheng, X. Sun, F. Xu, H. Yu and H. Peng, *Nat. Biomed. Eng.*, 2020, **4**, 159–171.

35 S. G. Lehmann, B. Gilbert, T. G. Maffeis, A. Grichine, I. Pignot-Paintrand, S. Clavaguera, W. Rachidi, M. Seve and L. Charlet, *Nanomaterials*, 2018, **8**, 232.

36 Y. Zhang, N. Zheng, Y. Cao, F. Wang, P. Wang, Y. Ma, B. Lu, G. Hou, Z. Fang, Z. Liang, M. Yue, Y. Li, Y. Chen, J. Fu, J. Wu, T. Xie and X. Feng, *Sci. Adv.*, 2019, **5**, eaaw1066.

37 H. Yang, Z. Qian, J. Wang, J. Feng, C. Tang, L. Wang, Y. Guo, Z. Liu, Y. Yang, K. Zhang, P. Chen, X. Sun and H. Peng, *Adv. Funct. Mater.*, 2022, **32**, 2204794.

38 K. Zeng, X. Shi, C. Tang, T. Liu and H. Peng, *Nat. Rev. Mater.*, 2023, **8**, 552–561.

This journal is © The Royal Society of Chemistry 2024

J. Mater. Chem. B, 2024, **12**, 5594–5599 | 5599